Nuclear Instruments and Methods in Physics Research A237 (1985) 366–380
North-Holland, Amsterdam

V. Undulator magnets and optics

PERIODIC MAGNETS FOR FREE ELECTRON LASERS

R.P. WALKER

SERC Daresbury Laboratory, Warrington WA4 4AD, UK

The design of periodic magnets or undulators for use in free electron lasers is reviewed. The application of electromagnet and permanent magnet technology for the construction of undulators with both planar and helical geometries is described and the performance of each type compared. Particular attention is given to the practical problems that are associated with the more popular permanent magnet devices. Reference is made to the undulators used in existing experiments, emphasising any novel features.

1. Introduction

In a free electron laser (FEL) the presence of a static periodic magnetic field produced by an undulator magnet allows energy from a beam of relativistic electrons to be used in amplifying coherent optical radiation. The interaction results from the transverse periodic motion or undulation induced in the electron trajectory by the magnetic field. FELs can be divided into two basic types, plane or helical, depending on the field configuration. In a plane periodic magnet the field has the form:

$$\boldsymbol{B} = B_0(0, \sin kz, 0),$$

where $k = 2\pi/\lambda_0$. This introduces a similar sinusoidal trajectory in the x–z plane and the radiation produced is plane polarized. In a helical magnet:

$$\boldsymbol{B} = B_0(\cos kz, \sin kz, 0).$$

The corresponding motion is helical and the radiation is circularly polarized. In both cases the maximum angle that the electron makes with the z-axis is given by K/γ and the amplitude of motion by $K/\gamma k$ where the important parameter K is defined by:

$$K = \frac{eB_0\lambda_0}{2\pi mc} = 93.4B_0[\mathrm{T}]\lambda_0[\mathrm{m}].$$

The basic operation of the FEL is the same in both cases leading to a resonant condition when the radiation wavelength, λ, and electron energy, γmc^2, satisfy the following:

$$\lambda = \frac{\lambda_0}{2\gamma^2}\left(1 + \frac{K^2}{2}\right), \tag{1}$$

in the case of a plane geometry. In the helical case $K^2/2$ is replaced by K^2.

2. FEL types

The two main quantities which characterize the performance of an FEL are the gain – the relative increase in radiation intensity at small signal levels – and the efficiency – the relative amount of energy that can be extracted from the electron beam when saturation has been reached. Since the first FEL experiment took place at Stanford [1,2] using a constant parameter undulator, i.e. one in which the magnet period and field amplitude is constant along the length of the device, a number of variations have been

0168-9002/85/$03.30

developed in order to improve the performance of the basic scheme. In the variable parameter or tapered undulator [3,4] the magnet parameters are profiled to match the desired decrease in the electron energy along the length of the magnet, i.e. γ, λ_0 and B_0 are regarded as functions of z in eq. (1). In this way a greater extraction efficiency can be obtained. This has been demonstrated in recent years by three successful single pass experiments in which an external laser beam was amplified [5–7]. The degree of taper used in these experiments varied between 2% and 9% in γ.

Another variation of the basic FEL is the optical klystron [8] which consists simply of two undulators separated by a dispersive section to increase the degree of bunching of the electron beam and hence the gain. Several devices of this kind have been developed at Novosibirsk [9–11]. The undulator magnet of the FEL experiment being mounted on ACO can also be arranged as an optical klystron and recently operation of the first storage ring FEL oscillator was reported with this configuration [12].

The operation of a tapered wiggler is only optimized at a given power level and so is not ideal in an oscillator configuration when a rapid build up of power is required. In order to overcome this problem and so produce a high power output oscillator a multicomponent design has been put forward [13] which includes a number of constant and tapered sections as well as a dispersion section as in an optical klystron. Such an arrangement has been designed for the TRW/Stanford experiment [14] and recently successful operation was reported [15].

Mention should also be made of another scheme in which an alternating transverse field gradient is superimposed on the periodic field in order to make the gain independent of electron energy over a broad range [16]. Although the theory for such a device is well developed [17] none so far have been built and so will not be considered further. Finally, a scheme has been put forward for producing radiation with arbitrary polarization using an arrangement similar to that of the optical klystron except that the undulators are placed with fields perpendicular rather than parallel to each other [18].

3. Choice of magnet parameters

Most of the present-day FEL experiments employ a plane magnet geometry rather than helical. The reasons for this are not related to FEL performance directly, rather they are based on technological grounds – experience to date shows that plane magnets are easier to construct and in general achieve higher field levels. They also provide easy access to the vacuum vessel so that viewing screens and pumping ports can be incorporated in the design. In particular all of the experiments using an optical klystron or a tapered undulator are based on plane polarization although the basic concept could be applied to the helical case also.

The choice of magnet parameters is first of all constrained by the desired operating wavelength and in experiments carried out to date by the energy of the available electron source. Optimization of parameters to produce, for example, maximum gain is in general very complex, mainly as a result of having to take into account the effects of finite electron beam emittance in which the magnet parameters also play a part. Often there is a desire to reduce the magnet period, partly because this allows a greater number of periods to be accommodated in a given length, but limitations are set by magnet technology, as will be discussed in section 4 and by the increasing effects of electron beam emittance. It may be desired to provide a certain tuning range for the output wavelength. This can be done by varying either the electron energy or the magnetic field amplitude. In the latter case it is clear from eq. (1) that higher values of K provide a greater tuning range. Large K values ($\gtrsim 2$) are also an advantage if operation on a higher harmonic is desired. As a result of the many factors that have to be taken into consideration it is not surprising that the K values used in current experiments vary over a wide range, 0.3–5.2 (see table 1). Magnet periods also vary over a wide range between 25 and 200 mm while field amplitudes vary between 0.05 and 0.7 T.

In an FEL it is important to control the electron beam trajectory carefully so as to optimize the physical overlap and hence coupling between the electron and photon beams. It is usual to design the magnet with zero field integral, $\int B_y \mathrm{d}z$, and with symmetry about the mid point so that there is no net displacement or angular change introduced by the magnet. This requires that there are "half poles" at either end

contributing half the field integral of the full poles. In addition attention must be paid to the quality of the field throughout the magnet. Non-periodicity, such as a random variation in peak field values for example, can introduce distortions in the trajectory. In order to achieve adequate uniformity it may be necessary therefore to incorporate in the design some means of trimming the field or to make provision for external correction windings.

4. Magnet technology

4.1. Plane electromagnets

In a plane electromagnet (see fig. 1) assuming poles wide enough to reduce the field to a two dimensional form, Maxwell's equations can be satisfied by the following expressions:

$$\begin{aligned} B_y &= \sum_{m \text{ odd}} B_m \sin(mkz)\cosh(mky), \\ B_z &= \sum_{m \text{ odd}} B_m \cos(mkz)\sinh(mky), \end{aligned} \tag{2}$$

where $k = 2\pi/\lambda_0$. As a boundary condition it may be assumed that the distribution of B_z at the magnet poles ($y = g/2$) is a square wave function [19]. The peak value is given by Ampère's law; taking a line integral around two coils, assuming infinite permeability in the steel gives:

$$B_z\lambda_0/4 = 2\mu_0(NI), \tag{3}$$

where (NI) is the number of ampere-turns per coil. Thus in eq. (2):

$$B_m = \frac{32\mu_0 NI}{\pi\lambda_0}\,\frac{\sin(m\pi/4)}{m\sinh(mkg/2)}.$$

It has been shown by comparison with the results of detailed computer calculations that good agreement can be obtained with two terms in eq. (2) [20]. Then the field under the pole is given by:

$$B_y = \frac{32\mu_0 NI}{\sqrt{2}\,\pi\lambda_0}\left[\frac{\cosh(ky)}{\sinh(\xi)} - \frac{\cosh(3ky)}{3\sinh(3\xi)}\right], \tag{4}$$

where $\xi = \pi g/\lambda_0$.

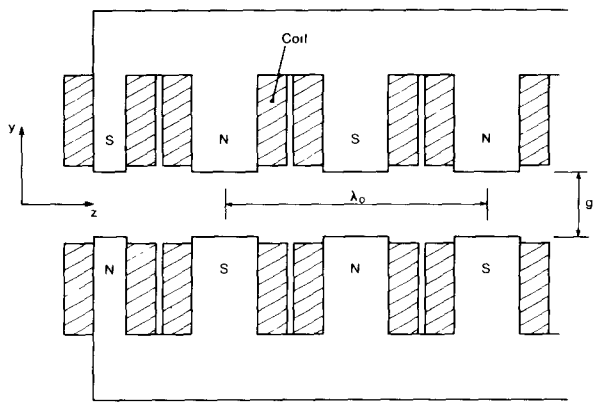

Fig. 1. Geometry of an electromagnetic plane periodic magnet.

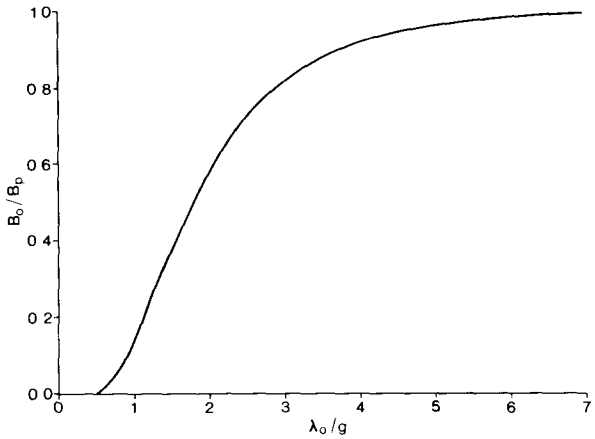

Fig. 2. Ratio of field amplitude on axis to field at pole tip as a function of ratio of magnet period to gap height, eq. (5).

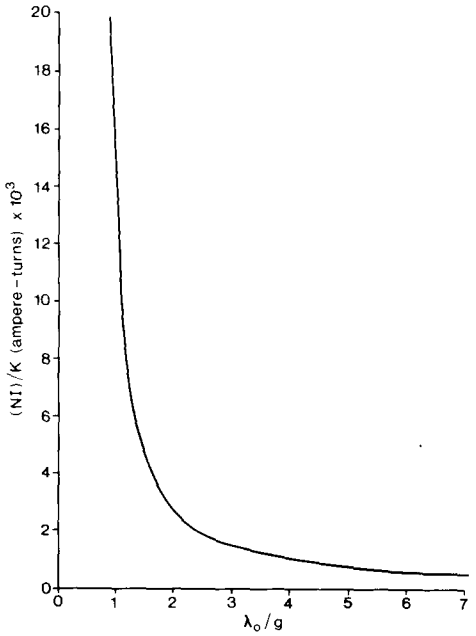

Fig. 3. Number of ampere-turns per coil required per unit K as a function of λ_0/g, eq. (6).

The variation in B_y across the magnet gap results in the maximum field on axis, B_0, being different to that at the pole tip, B_p:

$$B_0/B_p = \frac{1}{\cosh(\xi)}\left[\frac{1-\dfrac{\sinh(\xi)}{3\sinh(3\xi)}}{1-\dfrac{\tanh(\xi)}{3\tanh(3\xi)}}\right]. \tag{5}$$

It can be seen from fig. 2 that for a given maximum pole tip field and minimum gap B_0 decreases rapidly as the period is reduced and so the maximum achievable value of K decreases ever more rapidly. Eq. (4) can be re-arranged to give the following expression for the K value achievable with a given excitation:

$$K = 8.45 \times 10^{-4}(NI)\left[\frac{1}{\sinh(\xi)} - \frac{1}{3\sin(3\xi)}\right]. \tag{6}$$

The dramatic increase in the excitation required as λ_0/g decreases can be clearly seen in fig. 3, rising from nearly 3000 ampere-turns at $\lambda_0/g = 2.0$ to 14000 ampere-turns at $\lambda_0/g = 1.0$. Since the space between adjacent poles decreases with the period a situation is soon reached when the current density becomes so large that superconducting coils are needed even though the field on axis may be quite modest. For example, with a gap of 20 mm and for $K = 1$ the required current density rises from 10 A/mm^2 at $\lambda_0/g = 3.3$ to 100 A/mm^2 at $\lambda_0/g = 1.7$, assuming coils completely filling a square aperture between adjacent poles. In practice the situation is much worse since saturation in the magnet steel, which can be large in this type of magnet even with relatively small values of B_0, is not taken into account in the equations above.

The magnet for the LELA experiment at Frascati is a conventional electromagnet with relatively large period, 116 mm, and gap, 40 mm, ($\lambda_0/g = 2.9$) and which produces a field amplitude, B_0, of 0.48 T, giving $K = 5.2$ with 12600 ampere-turns per pole [21]. The current density was 30 A/mm^2. Measurements on the prototype showed that an increase of about 70% in the ampere-turns was required to overcome saturation

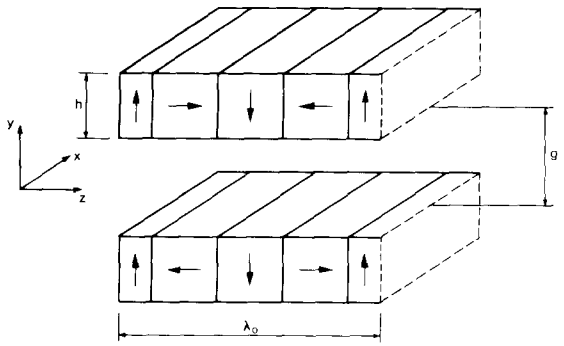

Fig. 4. Geometry of REC plane periodic magnet.

in the steel, but also that the end poles became saturated at lower current levels than the inner poles. The direct consequence of this was a variation of field integral with excitation level. This is a general problem for electromagnets which can only be overcome by the provision of separately controlled coils for the end poles. The magnet used in the first FEL experiments on the ACO storage ring had a much smaller period, 40 mm, and gap, 22 mm ($\lambda_0/g = 1.8$) [22]. In this case superconducting coils with a current density of 280 A/mm^2 were used to provide the 10000 ampere-turns required for the field amplitude of 0.45 T ($K = 1.68$), about twice the amount that would have been required in the absence of saturation [23].

4.2. Plane permanent magnets

The problem of achieving the required high current densities at small values of λ_0 in an electromagnet can be avoided by use of permanent magnets whose dimensions can be scaled while retaining the same field values. In particular rare-earth cobalt (REC) offers many advantages over older types of material, not just because of the high remanent field (0.8–1.0 T). REC has an almost linear demagnetisation curve with a slope of close to unity so that the material behaves like a vacuum with current sheets at the block surfaces. As a result the magnetic fields from individual pieces superpose linearly so that field distributions may be calculated relatively easily and in some cases analytic expressions can be derived. Other advantages are that pieces may be assembled without problems of demagnetisation and also that external fields for steering or focusing for example may be superposed on that of the REC itself. The properties of REC and its use in various types of magnetic element are discussed in refs. [24] and [25].

REC undulators have been pioneered at Stanford and Novosibirsk. In the first optical klystron constructued for the VEPP-3 storage ring at Novosibirsk iron pole pieces were used to overcome field inhomogeneities arising from the large spread in magnetisation strength of the individual blocks [10]. The design developed at Stanford by Halbach [26] on the other hand, contained REC material only and is shown in fig. 4. The first device of this type built for use at SSRL as a source of synchrotron radiation had a period of 61 mm and at minimum gap 27 mm produced a field amplitude of 0.28 T [27]. Since then many undulators have been built with this design for use as synchrotron radiation sources [28] and in FEL experiments.

The field distribution produced is shown in fig. 5 and is to a very good approximation sinusoidal on axis. The field amplitude for the case of infinitely wide blocks can be calculated analytically and is given by [26]:

$$B_0 = 2B_r \frac{\sin \epsilon\pi/M}{\pi/M}(1 - e^{-2\pi h/\lambda_0})\, e^{-\pi g/\lambda_0}, \tag{7}$$

where

B_r = remanent field,

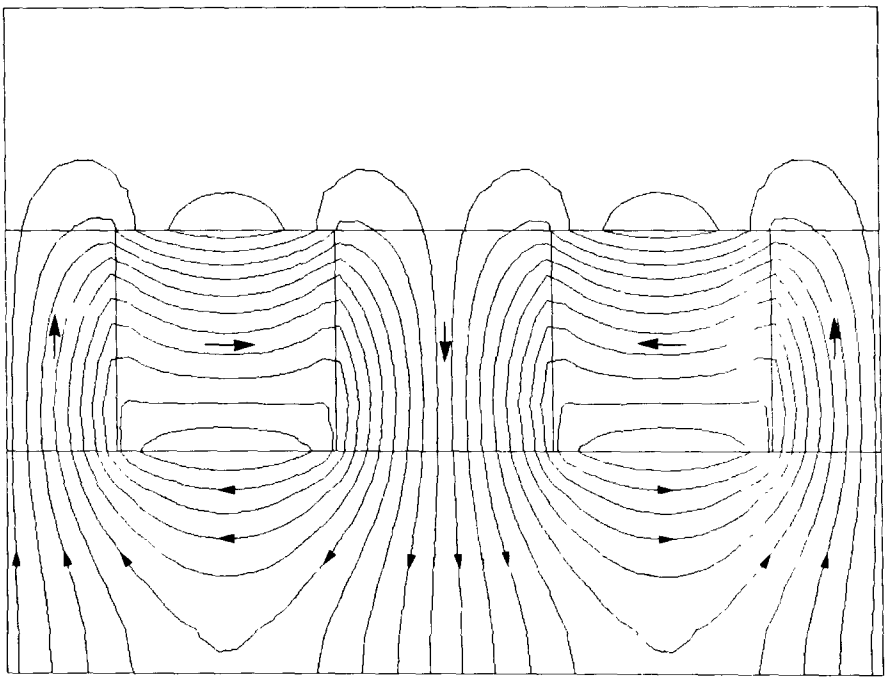

Fig. 5. Field lines in REC plane periodic magnet.

M = number of blocks per period,
h = block height,
ϵ = fill factor, to take account of spaces between the blocks.

A derivation is given in ref. [29]. It is most common to use four blocks per period ($M = 4$), as illustrated in fig. 4. The increase in field amplitude obtained with eight blocks per period is only 8%, assuming the same block height, and to achieve this involves magnetizing them along directions other than block edges which would lead to inhomogeneity in the strength of magnetisation. It is also convenient to use square cross-section blocks. Then with no spaces between blocks ($\epsilon = 1$) and $B_r = 0.9$ T eq. (7) gives:

$$B_0 = 1.284\, e^{-\pi g/\lambda_0}. \tag{8}$$

This shows that a K value of 1.0 is achievable with a gap of 20 mm and $\lambda_0/g = 2.0$. By doubling the height of the blocks ($h = \lambda_0/2$) about 20% extra field can be gained, however the increased cost and reduction in flexibility for block selection makes this an unattractive option.

The three dimensional field distribution may be calculated readily for such a geometry by summing the field from each block, which is given by [30]:

$$B_i = \frac{\mu_0}{4\pi} \sum_{\substack{j=1 \\ k \neq i \neq j}}^{3} \left[M_i \tan^{-1}\left(\frac{r_i r_k}{r_j r} \right) \right]_{r_{i1} r_{j1} r_{k1}}^{r_{i2} r_{j2} r_{k2}} + M_j \left[\ln(r_k + r) \right]_{r_{i1} r_{j1} r_{k1}}^{r_{i2} r_{j2} r_{k2}}. \tag{9}$$

In the above expression which is in a convenient form for including in a computer program indices i, j and k can take values 1, 2 or 3 representing the x, y or z vector components respectively. Such a program is useful for computing fringe field distributions and for assessing the effect of block magnetisation error as well as in determining the magnet width required to obtain a given field homogeneity, although an analytic solution has been put forward in the latter case [25].

The requirement for zero field integral is more easily met in this kind of magnet compared to an electromagnet; in fact the superposition property of REC means that use of end blocks of half length meets

the requirement exactly [31]. This scheme avoids the complication of a rotatable full block used in some designs and also has the advantage of being independent of gap setting. In practice however differences between the magnetisation strengths of half and full blocks may require some compensation by means of small trim coils.

One of the main drawbacks to the pure REC design is that the inevitable variation of magnetisation strength and direction from block to block produced by the manufacturing process reflects itself directly in the field distribution and hence can cause deviations in the electron beam trajectory. This has proved to be important in many current FEL experiments and is discussed further in section 5.

In the so-called "hybrid" design shown in fig. 6 steel poles are used in conjunction with REC material to produce larger field amplitudes. The performance can be estimated simply in the following way, based on the equations developed earlier for the electromagnet case. Assuming as before equal pole length and separation, infinite permeability in the steel and that the REC material nearest the axis is working at close to open-circuit conditions then B_z in eq. (3) becomes simply B_r (strictly $\mu_0 H_0$) and so the field amplitude becomes:

$$B_0 = \frac{4B_r}{\sqrt{2}\,\pi}\left[\frac{1}{\sinh(\xi)} - \frac{1}{3\sinh(3\xi)}\right]. \tag{10}$$

It can be seen from fig. 7 that the increase in field compared to a pure REC design with a similar large volume of REC material ($h = \lambda_0$) is 20% at $\lambda_0/g = 4$ but this reduces to zero at $\lambda_0/g = 2$. For comparison the results for a REC design with square cross-section blocks, eq. (8), is also shown. Another advantage of the hybrid design is that the peak field is less sensitive to variations in the angle of magnetisation of the REC. It is also possible to incorporate tuning studs to trim the field under the individual poles and so produce a very uniform field quality. A disadvantage however is the increased design effort required since the field distributions can no longer be calculated easily.

It is possible to increase the field amplitude further by reducing the pole length and using more REC

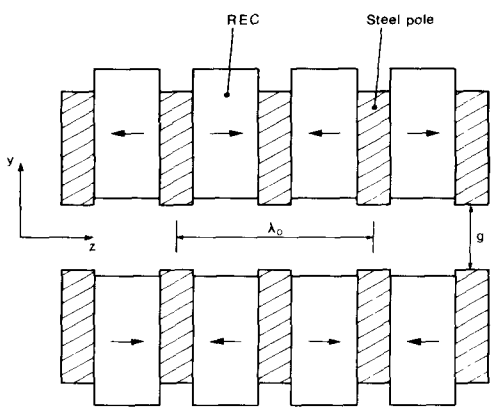

Fig. 6. Geometry of hybrid REC + steel plane periodic magnet.

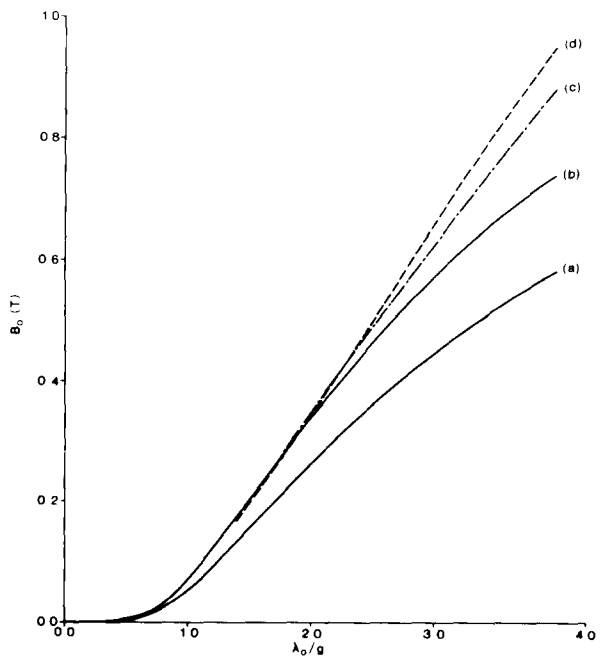

Fig. 7. Field amplitude in REC and hybrid magnets as a function of λ_0/g: (a) REC only, $h = \lambda_0/4$; (b) REC only, $h = \lambda_0$; (c) hybrid, eq. (10); (d) hybrid, eq. (11).

material between the poles. Halbach has carried out 2D magnetic field computations and found that after optimizing the pole length for a number of values of period/gap the data could be described accurately over the range $1.4 < \lambda_0/g < 14.0$ by the following expression [32]:

$$B_0 = 3.33 \exp\left[\frac{-g}{\lambda_0}\left(5.47 - 1.8\frac{g}{\lambda_0}\right)\right]. \tag{11}$$

This assumes use of REC with $B_r = 0.9$ T and high permeability (Vanadium–Permendur) steel. This result is also shown in fig. 7 and it can be seen that it deviates from eq. (10) by less than 10% over the range of interest. The main disadvantage of this approach is the increased proportion of higher harmonics and the corresponding increase in transverse field homogeneity [20].

Hybrid undulators have been built for FEL experiments with an optical klystron on VEPP-3 at Novosibirsk [10,11]. OK-2 had a period of 65 mm, a gap of 11 mm and produced a field amplitude of 0.7 T giving a relatively large K value of 4.2, while OK-3 had a period of 69 mm a gap of 13 mm and produced a field of 0.6 T ($K = 3.9$). The field levels in this case were about 50% of that predicted by eq. (11) however the strength of the REC material was smaller ($B_r = 0.83$ T, $\mu_0 H_c = 0.74$ T) and the volume of material less than that assumed in deriving eq. (11). In OK-2 each pole was supported by a vertical adjusting screw allowing the field to be altered by changing the gap. To localize the field variation thin iron liners were located between each half period connected to the iron foundation of the magnet. Further experience with hybrid magnets has been gained at synchrotron radiation laboratories. Here use is made of the fact that fields in excess of 2 T can be obtained if the ratio of period to gap is sufficiently large which makes them attractive for use as multipole wigglers. A device of this kind has been built and installed at SSRL, Stanford [33], for example. In this design the tuning studs alter the field by shunting flux between the top of adjacent poles. Similar magnets are also being studied at NSLS, Brookhaven [34].

4.3. Helical magnets

A circularly polarized transverse field is produced by two identical coaxial solenoids separated by half the pitch of the coils λ_0, carrying current, I, in opposing directions in order to cancel the axial field component. The amplitude of the transverse field is given by:

$$B_0 = 8\pi 10^{-7}\frac{I}{\lambda_0}\left[\xi K_0(\xi) + K_1(\xi)\right],$$

with $\xi = \pi g/\lambda_0$, where g is the internal diameter, K_0, K_1 = modified Bessel functions. This shows a rapid decrease in B_0 as λ_0/g reduces, analogous to the behaviour of plane electromagnets and permanent magnets. An approximation which is good to 10% for $\xi > 1$ allows the following expression to be derived for a sinusoidal current distribution [35]:

$$K = 3.80 \times 10^{-4} I\, e^{-0.9\xi}. \tag{12}$$

Thus for $K = 1$ the current required increases from 11 000 A to 44 000 A as λ_0/g decreases from 2.0 to 1.0. These values are between 1.5 and 2 times greater than the corresponding figures for a plane electromagnet. The expression above is valid for an infinitesimal current sheet but may be generalised easily for finite coil thicknesses. For example, with a square cross-section coil of side $\lambda_0/4$ the result is an equation of the same form as eq. (12) above but with a numerical constant of 2.03×10^{-4}, i.e. the field is reduced by a further factor of about 2 in this case. Roughly speaking therefore the helical electromagnet is between 3 and 4 times less efficient in producing field than the plane electromagnet for the same aperture.

As a result of the lower field capability and the increased technical complexity fewer helical magnets have been built compared with the alternative plane geometry. The superconducting helical magnet for the Stanford FEL experiment had a period of 32 mm, internal coil diameter of 11 mm and achieved a peak field amplitude of 1.3 T when operated at a current level of 700 A/mm^2 [36]. Under normal operating conditions however the field level was about 0.2 T. A pulsed helix is used as part of the FEL experiment at

ENEA, Frascati [37]. This has a period of 24 mm, internal diameter of 20 mm and at 3.6 kA achieves a peak field of 0.22 T ($K = 0.5$). It is planned to replace this in the near future however with a plane permanent magnet undulator.

The poor performance of the helical magnet design described above compared to a plane electromagnet is of course due to the fact that there is no iron in the structure. Iron poles can be used to enhance the field, as has been done at Novosibirsk in a magnet installed in the VEPP2 ring for high energy physics use. Fields of 0.2 T were achieved with a period of 24 mm and internal diameter of 15 mm. Extremely high current densities were employed, about 200 A/mm^2, and the helical steel geometry added after the coil had been wound enhanced the field by about a factor of 2. For the FEL experiment at Bell Telephone Laboratories a novel scheme was devised in which the iron poles were fed by straight rather than helical current leads. The conductor could therefore have a larger cross-section in order to reduce the power consumption [38]. A prototype with 200 mm period and 120 mm internal diameter generated a peak field of 0.043 T ($K = 0.8$) with an excitation of 9 kA in a conventional coil.

A helical magnet with better performance can in principle be achieved using REC material. The design suggested in ref. [25] uses a number of "slices" of dipole magnet, such as the one shown in fig. 8 composed of M blocks, arranged along the length of the undulator with a $2\pi/N$ rotation between each slice. The field level achievable with such an arrangement is given by:

$$B_0 = B_r \frac{\sin \pi/N}{\pi/N} \frac{\sin 2\pi/M}{2\pi/M} [T(x_1) - T(x_2)],$$

where $T(x) = K_0(x) + (x/2)K_1(x)$ and $x = 2\pi r/\lambda_0$. K_0, K_1 are modified Bessel functions. For $x > 1.0$, i.e. $\lambda_0/g < \pi$, it appears that $T(x)$ can be approximated by:

$$\ln T(x) \simeq 0.5 - 0.95x,$$

from which it follows that:

$$B_0 \simeq 1.649 B_r \frac{\sin \pi/N}{\pi/N} \frac{\sin 2\pi/M}{2\pi/M} e^{-0.95\pi g/\lambda_0} [1 - e^{-0.95(2\pi h/\lambda_0)}],$$

which is of a similar form as eq. (7) with block "height" $h = r_2 - r_1$. In particular with $N = 4$, $M = 8$, $h = \lambda_0/4$ and $B_r = 0.9$ T the field is given by:

$$B_0 \simeq 0.932 e^{-0.95\pi g/\lambda_0}. \tag{13}$$

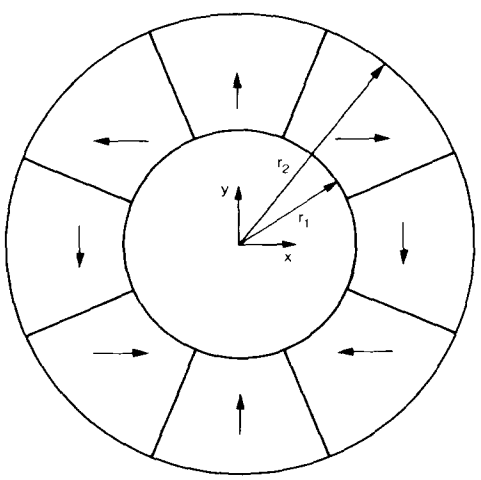

Fig. 8. Geometry of REC helical magnet.

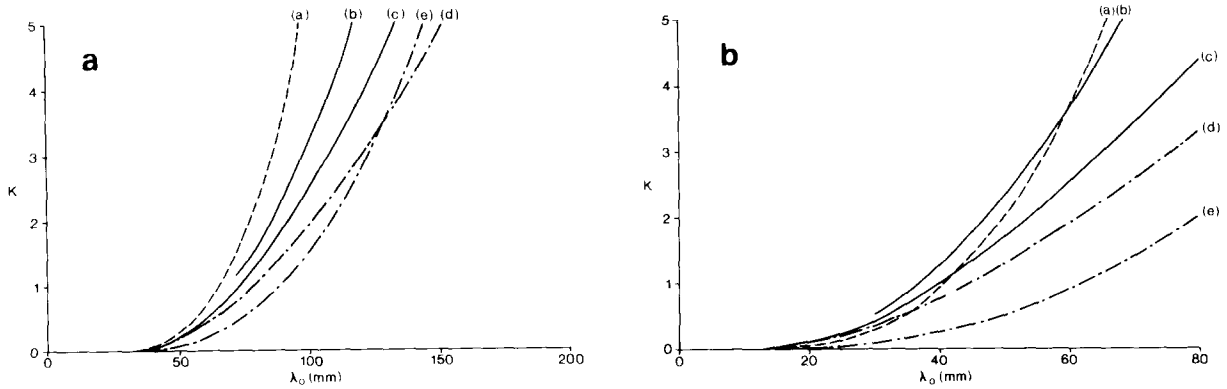

Fig. 9. Maximum K value achievable for various periodic magnet types as a function of magnet period (a) gap = 50 mm, (b) gap = 20 mm, (a) plane electromagnet, (b) plane hybrid, (c) plane REC, (d) helical REC, (e) helical electromagnet.

By comparison with eq. (8) it can be seen that similar field levels can be achieved to the plane REC geometry. Using the same example $K = 1$ can be obtained at $g = 20$ mm with $\lambda_0/g = 2.2$. There is increasing interest in this type of magnet but none have yet been built. Originally use of trapezoidal shaped blocks was suggested [25] but recently a simple method of producing blocks with the required directions of magnetisation has been put forward [39] while another study has shown that a design based on the use of a large number of small rectangular blocks with equal magnetisation can produce acceptable field quality [40].

4.4. Comparison of magnet performance

In figs. 9a and 9b the magnetic field performance of various types of undulator are compared, summarizing the discussions in the previous sections. The maximum achievable K value is given as a function of magnet period at fixed gap settings of 20 mm and 50 mm. The plane and helical electromagnets (curves a and e respectively) have a current density of 50 A/mm^2 in coils which have a square cross-section with side $\lambda_0/4$. In the case of an electromagnet therefore the coils fill the available space between the poles. The pure REC plane undulator (curve c) is given by eq. (8), the hybrid (curve b) by the empirical result of eq. (11) and the REC helix (curve d) by eq. (13). It can be seen that at smaller values of λ_0/g the REC and hybrid undulators compare favourable with the electromagnet, particularly at the smaller gap. The electromagnetic helix performance is poor by comparison with the plane device, however the REC helix achieves comparable performance to the REC plane magnet.

5. Construction and performance of permanent magnet undulators

The majority of present day FEL experiments employ a plane undulator geometry and the magnets are constructed using rare earth cobalt material. In this section some further practical details associated with these devices are presented.

5.1. Magnetic performance

Most groups have performed some form of magnetic measurements on the individual blocks to determine the variation in strength and angle of magnetisation so that the effect on the electron beam trajectory could be assessed. The measurements have been made in a variety of ways, the most popular being the use of a Hall plate to take a number of point readings. In the simplest case readings taken above and below the block centre give the magnetisation strength in the vertical direction. The other components

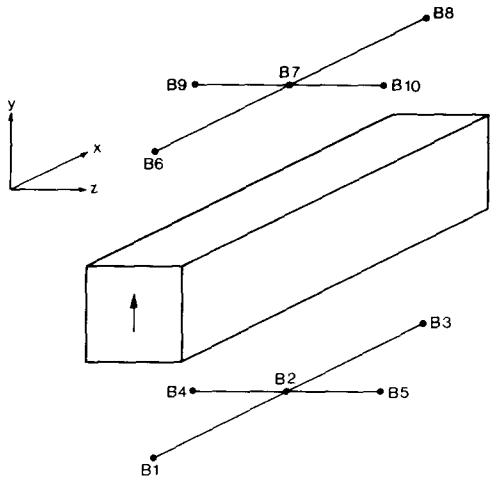

Fig. 10. Scheme for magnetic measurements on REC blocks.

can be obtained by measuring a single field component at a number of other points around the block. For example, using the readings of B_y taken at the points indicated in fig. 10 enables the magnetisation components and block centre offsets, representing the inhomogeneity of the block, to be determined as followed [31]:

$$M_x = \frac{B1 - B3 - B6 + B8}{4C_1}, \quad M_y = \frac{B2 + B7}{2C_2}, \quad M_z = \frac{B4 - B5 - B9 + B10}{4C_3},$$

$$4C_1,$$

$$\Delta_x = \frac{B1 - B3 + B6 - B8}{4M_yC_4}, \quad \Delta y = \frac{B2 - B7}{2M_yC_5}, \quad \Delta z = \frac{B4 - B5 + B9 - B10}{4M_yC_6}.$$

The coefficients C_1–C_6 can be found easily in any given case by calculating the field produced at the relevant points by blocks with the magnetisation vector aligned along the x, y or z direction using eq. (9). The block must be located accurately in position and angle with respect to the probe, however systematic errors can be removed by measuring with the same block in different orientations. In another technique [41] the block to be measured and a reference block were spun inside a coil and the output voltage recorded. In this case the block was modelled by a magnetic dipole at the block centre and the different values obtained after making various changes to the orientation of the block were interpreted as angular and position errors of the dipole.

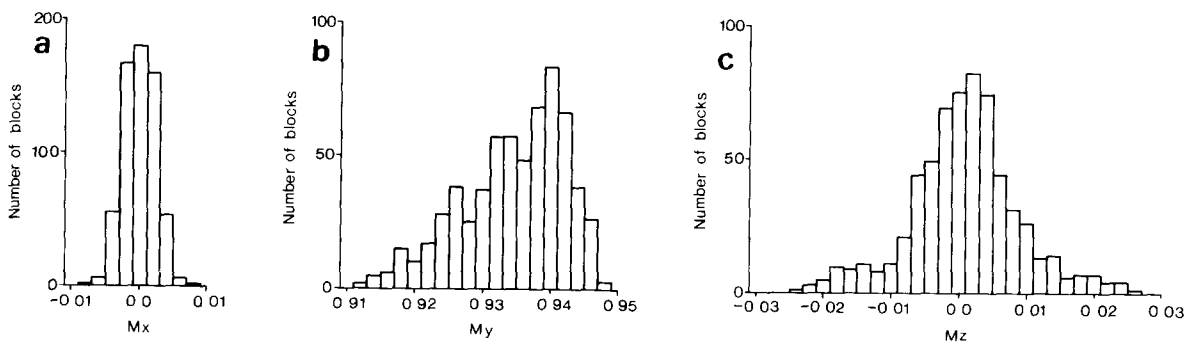

Fig. 11. Distributions of magnetisation in the x, y, z directions.

Fig. 11 shows the distributions of magnetisation errors obtained after measuring 600 blocks for the UK FEL project [42]. The M_y distribution is asymmetric with a mean of 0.934 T and a full spread of $\pm 1.9\%$. This is very similar to the result obtained by the MSNW team [43] and agrees with the total width measured by the NSLS group, however in the latter case the distribution is quite different having two peaks [41]. The full range of M_x and M_z values corresponds to errors in the magnetisation direction of about $\pm 0.4°$ and $\pm 1.3°$ respectively. MSNW obtained similar sized errors for M_z however larger errors were seen in M_x, $\pm 2°$ being typical. Measurements on the NOEL undulator showed larger errors also, $\pm 2\%$ in strength (fwhm) and $\pm 2°$ in M_x (fwhm) [44]. The results obtained at Los Alamos showed a similar spread in magnetisation strength but unusual behaviour was observed in the measured values of Δy [45].

The important errors in determining the electron trajectory are those in M_x and M_y for which $\int B_x \mathrm{d}z$ and $\int B_y \mathrm{d}z$ respectively are non-zero, since these result in angular shifts in the vertical and horizontal plane. A simple estimate can be made of the magnitude of error in position and angle after traversing a magnet:

$$\sigma_x = \sqrt{2}\,\frac{\lambda_0}{4}\sigma_\theta \left[\sum_{i=1}^{N/2} i^2\right]^{1/2}, \quad \sigma_{x'} = \sqrt{N}\,\sigma_\theta, \tag{14}$$

where N is the total number of blocks in the magnet and σ_θ is the rms angular error introduced by a single block, related to the rms spread in field integral and hence magnetisation. Identical expressions hold also for the y-motion. The magnitude of the error increases when the electron energy is reduced however in proportion to the amplitude and maximum angle of the ideal trajectory it remains the same. For the UK FEL blocks the field integrals are given by:

$$\int B_x \mathrm{d}z = 17.6 \times 10^{-4} M_x, \quad \int B_y \mathrm{d}z = 18.3 \times 10^{-4} M_y,$$

and hence at the 50 MeV operating energy with the measured rms M_x and M_y errors of 0.0110 and 0.0023 respectively the angular shifts (σ_θ) are 0.12 mrad and 0.024 mrad. Using eq. (14) above with $N = 152$ and $\lambda_0 = 65$ mm results in the following errors:

$$\sigma_x = 1.1 \text{ mm}, \quad \sigma_{x'} = 1.5 \text{ mrad},$$
$$\sigma_y = 0.2 \text{ mm}, \quad \sigma_{y'} = 0.3 \text{ mrad}.$$

These values which were confirmed by tracking studies were considered unacceptable and led to the development of a method of compensation in common with other FEL groups.

Various schemes have been devised for arranging the blocks in an undulator in such a way as to compensate for magnetisation errors [41,42,44,45]. The details of the methods vary since they are related to the information obtained from magnetic measurements which is different in each case. One scheme basically involves a pairing procedure: the blocks are ordered from small to large error and pairs formed by taking blocks from either end of the distribution. The procedure is repeated using the net error for a group of blocks. Another scheme is based on the trajectory error introduced. Starting at the entrance of the magnet and working towards the exit the blocks are selected to minimise the cumulative error in $(M_x^2 + M_y^2)$ – where the components refer in this case to the undulator coordinate system rather than that of the measurement system.

Measurements on completed undulators indicate that acceptable electron trajectories can be obtained after carrying out such a selection procedure. However most designs also include a number of individually powered trim coils along the length of the magnet for beam steering. At MSNW a floating wire technique was used to show that the maximum deviation in the x–z plane was 0.2 mm, however measurements in the uncorrected y–z plane gave errors of up to 2 mm requiring correction with trim coils [46]. At ACO a Hall probe was used to measure B_x and B_z distributions in addition to B_y and the results showed that these components were less than 2% of the sinusoidal field amplitude [44]. Problems were experienced however with the UCSB undulator [47]. A large spread in B_0 values of 2.5% rms was measured, B_z values were

larger than expected and in addition the distribution $B_1(x)$ did not show the expected quadratic dependence. It was suggested that bending of the magnet bars may have been responsible for the latter and a poor selection procedure for the former.

5.2. Engineering considerations

REC is a very brittle material and magnetic forces between blocks are in general very large [31] so that careful handling is required at all stages to prevent chipping or complete breakage. It is not desirable to carry out a great deal of machining on the pieces and in particular not in the region closest to the electron beam. The problem of attaching the blocks to a support structure has been tackled in various ways. The most popular seems to be to glue individual blocks into aluminium or stainless steel holders which can then be attached by bolts [42] or clamps [48] or can be slotted [43] into the baseplate. In one case the ends of the blocks had two perpendicular grooves machine in them [49]. The blocks were positioned along the length of the magnet by a toothed spacer bar which meshed with one set of grooves and a spline was inserted along the other groove to hold the blocks in place. In another scheme steps were cut into the side face of each block and clamps used to attach the blocks directly to a support frame [41]. In most cases the blocks have been attached singly allowing easier replacement in case of damage or re-configuration. Although REC blocks can be supplied with small dimensional tolerances it may still be desirable in some cases to leave spaces between the blocks to take account of the variation in size so that the peridocity can be accurately maintained.

The usual method of providing a variable field amplitude is to incorporate control of the gap between the magnet arrays. The forces between the arrays are however generally large so that careful mechanical design is necessary to meet the required parallelism between the arrays and setting accuracy. An illustration of the accuracy required is given by the relative change of field amplitude with gap, $\pi g/\lambda_0$, which for example is 10% per mm for a magnet period of 30 mm. The force is also non-linear, increasing rapidly at small separations, and for this reason incorporation of springs to help linearise the force may be desirable. The problems undoubtedly become greater as the magnet length increases. In the case of the UK FEL project it was decided to build the 5 m long magnet in 4 sections for this reason and also to ease handling and magnetic measurement. The solution adopted was to use half blocks at the ends of each section giving the added advantage that each section could be operated independently [42]. In this way there is no limitation on the length of magnet that can be built.

Tapered undulators are constructed in a similar fashion. In one scheme the magnetic period varies along the length of magnet and the blocks are therefore simply positioned with the required spacing. It is appropriate in this case to slot the blocks into position enabling a more rapid change of taper if required. The MSNW [43] and Los Alamos [49] undulators were constructed in this way with a 13% and 12% reduction in λ_0 along the length of the magnet respectively. The TRW undulator on the other hand had a fixed period and the taper was set by adjusting the length of spacer rods separating the two arrays [50]. The magnet was constructed in 5 sections each of which could be tapered individually. In the present multicomponent device the gap at either end of a section can be controlled independently by means of stepping motors enabling any desired taper to be quickly set up [51].

It is clear from eq. (7) and fig. 9 that the peak field obtainable depends critically on the minimum gap that can be used after making allowance for the electron and photon beam sizes. In some cases it is desirable therefore to minimise the gap by placing the REC arrays inside the vacuum vessel. Initially there were doubts about the suitability of REC, which is a sintered compound, in a high vacuum system. Tests however have been carried out which indicate that there are no problems [28,45]. The undulators for the Los Alamos and NSLS experiments for example are both in-vacuum, however in the latter case the REC blocks are contained within a thin can to prevent gas desorption by synchrotron radiation [52].

6. Conclusion

The use of rare earth cobalt permanent magnet technology has now become established as the more common means of construction of plane periodic magnets. In particular it has allowed magnets with small

Table 1
Main parameters of FEL undulators. R = rare earth cobalt, E = electromagnet, S = superconducting, P = plane geometry, H = helical geometry, T = tapered.

Experiment	L (m)	N	λ_0 (mm)	g (mm)	B_0 (T)	K	Type	Ref.
ACO I	0.92	23	40.0	22.0	0.45	1.7	S–P	[22,23]
ACO II	1.33	17	78.0	33.0	0.31	2.3	R–P	[44,48]
Bell	10.0	50	200.0	120.0	0.05	1.0	E–H	[38]
ENEA, Frascati I	1.25	52	24.0	20.0	0.22	0.5	E–H	[37]
ENEA, Frascati II	2.25	45	50.0	13.0	0.60	2.8	R–P	[37]
Los Alamos I	1.0	40	27.0	8.8	0.31	0.8	R–P–T	[45,49]
LELA	2.32	20	116.0	40.0	0.48	5.2	E–P	[21]
MSNW	2.31	97	25.4	12.7	0.26	0.6	R–P–T	[43]
Novosibirsk, OK-1	0.30	3	100.0	11.0	0.30	2.8	R–P	[9,10]
Novosibirsk, OK-2	0.33	4.5	65.0	11.0	0.70	4.2	R–P	[10,11]
Novosibirsk, OK-3	0.82	11	69.0	13.0	0.60	3.9	R–P	[11]
NSLS	2.6	40	65.0	10.0	0.70	4.3	R–P	[41]
Stanford	5.17	160	32.3	12.5	0.24	0.7	S–H	[36]
TRW I	2.67	75	35.6	15.0	0.27	0.9	R–P–T	[50]
UCSB	5.76	160	36.0	30.0	0.076	0.3	R–P	[47]
UK	4.94	76	65.0	22.0	0.46	2.8	R–P	[42]

period and gap to be constructed relatively easily which could only be achieved with great difficulty with an electromagnet and possibly only using superconducting technology. Problems associated with handling the brittle and strongly magnetic material have been overcome and several successful methods of construction have been devised including automation of the magnet gap to provide variable field amplitude. There are particular advantages in using REC in a tapered undulator. The blocks are usually positioned independently so that any desired tapering of magnet period is easily achieved. A linear tapering of magnet gap can also easily be provided. Problems arising from variations in the magnetic properties of the blocks are now understood and methods of testing the blocks and of arranging the blocks in the undulator to compensate for the errors have been devised. The use of REC in helical magnets has not yet been fully explored but seems an attractive possibility, overcoming many of the disadvantages of electromagnets as in the case of the plane geometry.

In the future magnets with even smaller periods and longer lengths than those used at present may be required for FEL experiments in the VUV or soft X-ray wavelength region. With permanent magnet devices there is in principle no problem, however to achieve a reasonable K value the magnet gap will have to be decreased also requiring a design in which the magnetic structure is located within the vacuum vessel. The hybrid scheme may be useful for such a device since this removes the need to accurately measure a large number of individual blocks. In all cases however magnetic measurement systems will have to be quite sophisticated to allow field values to be obtained with sufficient accuracy and with sufficient position resolution that electron trajectory errors can be determined and field tuning carried out.

The author is indebted to M.W. Poole for many helpful comments and suggestions.

References

[1] L.R. Elias et al., Phys. Rev. Lett. 36 (1976) 717.
[2] D.A.G. Deacon et al., Phys. Rev. Lett. 38 (1977) 892.
[3] N.M. Kroll, P.L. Morton and M.N. Rosenbluth, in: Physics of Quantum Electronics, vol. 7 (Addison-Wesley, Reading, MA, 1980) p. 89.
[4] N.M. Kroll, P.L. Morton and M.N. Rosenbluth, IEEE J. Quantum Electron. QE-17 (1981) 1436.
[5] H. Boehmer et al., Phys. Rev. Lett. 48 (1982) 141.
[6] W.E. Stein et al., Proc. 1981 Linear Accelerator Conf., Santa-Fe, NM (1981) Los Alamos Nat. Lab. Rep. LA-9234 (1982).

[7] J.M. Slater et al, IEEE J. Quantum Electron. QE-19 (1983) 374.
[8] N A. Vinokurov and A.N. Skrinsky, Institute of Nuclear Physics, Novosibirsk Preprint 77-59.
[9] A.S. Artamonov et al., Nucl. Instr. and Meth. 177 (1980) 247.
[10] G.A. Kornyukhin et al, Nucl. Instr. and Meth 208 (1983) 189
[11] G.A Kornyukhin et al., Institute of Nuclear Physics, Novosibirsk, Preprint 83-137.
[12] M. Billardon et al., Free-Electron Generators of Coherent Radiation, eds., C.A. Brau et al., SPIE 453 (1984) 269.
[13] M Z. Caponi and C.C. Shih, Phys. Rev. A26 (1982) 2285
[14] C.C. Shih and M.Z. Caponi, IEEE J. Quantum Electron. QE-19 (1983) 369.
[15] J.A Edighoffer et al., Phys. Rev. Lett. 52 (1984) 344.
[16] T.I Smith et al., J. Appl. Phys. 50 (1979) 4580.
[17] N.M. Kroll et al., IEEE J. Quantum Electron. QE-17 (1981) 1496.
[18] K.J. Kim, Lawrence Berkeley Lab. LBL 16640.
[19] S. Krinsky, Brookhaven Nat. Lab. BNL 23747.
[20] M.W Poole and R.P. Walker, Nucl. Instr. and Meth. 176 (1980) 487.
[21] R. Barbini et al., Nucl. Instr. and Meth. 190 (1981) 159.
[22] M. Bazin et al., Nucl. Instr. and Meth. 172 (1980) 61
[23] J. Perot and M. Lemonnier, Proc. Wiggler Meeting, Frascati, eds., A. Luccio et al. (INFN, Frascati, December 1978) p. 81.
[24] K. Halbach, Nucl. Instr. and Meth. 169 (1980) 1
[25] K. Halbach, Nucl. Instr. and Meth. 187 (1981) 109.
[26] H. Winick and J.E. Spencer, Nucl. Instr. and Meth. 172 (1980) 45.
[27] K. Halbach et al., IEEE Trans. Nucl. Sci. NS-28 (1981) 3136.
[28] G. Brown et al., Nucl. Instr. and Meth. 208 (1983) 65.
[29] M.W. Poole and R.P. Walker, IEEE Trans. Magn. MAG-17 (1981) 1978.
[30] M.W. Fan, M W. Poole and R.P. Walker, Daresbury Laboratory DL/SCI/TM29A (1981)
[31] R.P. Walker, M.W. Poole and D.G. Taylor, J Physique Coll Cl, 45 (1984) 321.
[32] K. Halbach, J. Physique Coll. Cl 44 (1983) 211.
[33] E. Hoyer et al., IEEE Trans. Nucl. Sci. NS-30 (1983) 3118.
[34] H. Hsieh et al., Nucl. Instr. and Meth. 208 (1983) 79.
[35] J.P. Blewett and R. Chasman, Stanford Synchrotron Radiation Project report 77/05 (May 1977) p. II-61.
[36] L.R. Elias and J.M. Madey, Rev. Sci. Instr 50 (1979) 1335.
[37] U. Bizzarri et al., J. Physique Coll Cl, 44 (1983) 313.
[38] E.D. Shaw, R.M. Emanuelson and G.A. Herbster, J. Physique Coll. C1, 44 (1983) 153.
[39] M.S. Curtin et al., these Proceedings (1984 FEL Conf., Italy) Nucl. Instr. and Meth. A237 (1985) 395.
[40] P Diament, these Proceedings (1984 FEL Conf., Italy) Nucl. Instr. and Meth. A237 (1985) 381.
[41] A.U. Luccio, P. Mortazavi and L.M. Yu, Nucl. Instr. and Meth. 219 (1984) 213.
[42] M.W. Poole, R.J. Bennett and R.P. Walker, J. Physique Col. Cl, 45 (1984) 325.
[43] J.M. Slater et al., J. Physique Coll. C1, 44 (1983) 73.
[44] J.M. Ortega, C. Bazin and D.A.G. Deacon, J. Appl. Phys. 54 (1983) 4776.
[45] R W. Warren, Los Alamos Nat. Lab. LA-UR-80-3677.
[46] D.C. Quimby, J. Appl. Phys. 53 (1982) 6613.
[47] L.R. Elias et al., Free-Electron Generators of Coherent radiation, eds., C.A. Brau et al., SPIE 453 (1984) 160
[48] J.M. Ortega et al., Nucl. Instr. and Meth. 206 (1983) 281.
[49] R.W. Warren et al., in: Physics of Quantum Electronics, vol. 8, (Addison-Wesley, Reading, MA, 1982) p. 397.
[50] H. Boehmer et al., ibid., p. 367.
[51] J.A. Edighoffer et al., Free-Electron Generators of Coherent Radiation, eds., C A. Brau et al., SPIE 453 (1984) 172.
[52] A.U Luccio, private communication.